doi:10.2533/chimia.2018.418 Chimia 72 (2018) 418–423

Enantiosensitive Bonding of Chiral Molecules on a Magnetic Substrate Investigated by Means of Electron Spectroscopies

Francisco J. Luque[a], Miguel Á. Niño[b], Michael J. Spilsbury[a], Iwona A. Kowalik[c], Dimitri Arvanitis[d], and Juan J. de Miguel*[aef]

Abstract: The adsorption of purely organic chiral molecules on ferromagnetic Co thin films is studied under ultra high vacuum conditions by means of synchrotron radiation-based electron spectroscopies, namely X-ray absorption and ultraviolet photoemission. X-ray absorption reveals that enantiomers with opposite handedness (*R*,*R*)– and (*S*,*S*)– of two different molecules adsorb with different strength on the Co surfaces and their valence band photoemission spectra also display distinctive features. In view of the recent reports describing the chiral-induced spin selectivity (CISS) effect these results lead us to consider the possibility that some enantiosensitivity may appear when bonding chiral molecules to a substrate with an initial asymmetry in the population of the different spin orientations.

Keywords: Adsorption · Chirality · Electron spectroscopy · Magnetism · Spin polarization

Francisco J. Luque is currently finishing his PhD at the Department of Condensed Matter Physics of the Univ. Autónoma de Madrid, Spain, under the supervision of Dr. Juan J. de Miguel. He holds a BSc in Physics from the University of Granada. His thesis research has been focused on the use of synchrotron radiation-based electron spectroscopies for the investigation of spin-related properties of molecular systems.

Miguel Ángel Niño is a scientist at IMDEA Nanoscience institute in Madrid (Spain). He earned his MS degree in 1997 from University of Granada, and in 2006 he received his PhD degree in Physics from the Department of Condensed Matter Physics, Universidad Autónoma de Madrid (Spain). After that he worked at the Nanospectroscopy beamline of Elettra Synchrotron in Trieste (Italy). His current research interests are the study of molecule/surface interfaces, prebiotic and catalytic chemical reactions on surfaces, and on magnetism of thin films and nanostructures.

Michael J. Spilsbury is currently a PhD student at the Department of Condensed Matter Physics of the Univ. Autónoma de Madrid, Spain, under the supervision of Dr. Juan J. de Miguel, working on the use of electron spectroscopies to investigate the properties of organic chiral molecules adsorbed on solid surfaces. He holds degrees in Electrical (2006) and Mechanical Engineering (2011) and a MS in Physics (2016) from the National Autonomous University of Honduras.

**Correspondence*: Dr. J. J. de Miguel[aef]
E-mail: juanjose.demiguel@uam.es
[a]Departamento de Física de la Materia Condensada, Universidad Autónoma de Madrid
28049-Madrid, Spain
[b]IMDEA-Nanoscience
Cantoblanco, 28049 Madrid, Spain
[c]Institute of Physics, Polish Academy of Sciences
02668-Warsaw, Poland
[d]Department of Physics and Astronomy
Uppsala University, 75237-Uppsala, Sweden
[e]Institute of Materials Science 'Nicolás Cabrera'
Universidad Autónoma de Madrid
28049-Madrid, Spain
[f]Institute of Condensed Matter Physics (IFIMAC)
Universidad Autónoma de Madrid
28049-Madrid, Spain

Iwona A. Kowalik is an associate professor at the Institute of Physics of the Polish Academy of Sciences in Warsaw. She received her PhD in Physics in 2006 studying magnetic semiconductors by means of photoemission spectroscopy. She has worked as a Post-Doctoral Fellow at MAX-lab synchrotron laboratory in Lund (Sweden), taking part in the commissioning of the soft X-ray beamline (I1011) for magnetism investigations. Her research interests include the understanding of the electronic and magnetic structure of modern functional spintronic materials investigated by synchrotron radiation techniques.

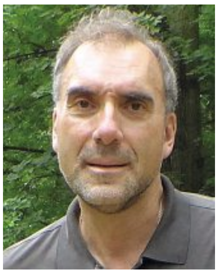

Dimitri Arvanitis is a senior lecturer at the Department of Physics and Astronomy of Uppsala University, Sweden. He received his PhD in 1988 and his habilitation in 1993 from the Freie Universität Berlin, Germany. His research is focused in the areas of surface science, nanoscience and magnetism, using core level spectroscopy at synchrotron radiation laboratories. He has participated in the design and buildup of the I1011 beamline of MAX-lab (Lund, Sweden), dedicated to the characterization of magnetic materials in the soft X-ray domain by dichroic core level spectroscopy.

Juan J. de Miguel is an associate professor at the Department of Condensed Matter Physics of the University Autónoma de Madrid (UAM). He obtained his PhD in Physics from UAM in 1989 and after that was a post-doctoral researcher at the University of Wisconsin-Madison (USA). His background is on surface physics and low-dimensional magnetism, and his current interests focus on magnetic nanostructures and molecular magnetism for spintronics applications.

1. Introduction

Chiral molecules appear in two different forms called *enantiomers* or *stereoisomers* that are mirror images of each other. In principle, their physico-chemical properties are expected to be practically identical. Nevertheless, all living organisms known to date use only one of the two chiral forms: left-handed (L) amino acids and right-handed (D) sugars.[1] The use of the opposite enantiomers for bio-medical applications can entail high risks, and for this reason the pharmaceutical industry faces a big challenge to develop methods that allow only the desired stereo-isomer to be obtained. Most chemical synthesis procedures yield both enantiomers with equal probabilities (a *racemic* mixture). Their separation and purification is a difficult and costly process called *chiral resolution*. Devising methods that allow for quick and efficient recognition of the different helicities of individual molecules and provide an easy way to separate them is therefore of great interest for industrial applications.

An attractive approach might be to develop media displaying enantioselective adsorption characteristics, and for this purpose we turn to magnetic materials. The relationship between molecular chirality and magnetism has been a matter of debate ever since Pasteur discovered the existence of chiral molecules in the XIX century. Nowadays it appears clearly established that chiral asymmetries in physico-chemical processes can only appear when they take place in a true chiral environment.[2] Magnetic fields can be used to establish chirality under specific conditions: for instance, magneto-chiral dichroism,[3] that is, the different absorption of light by a system of chiral molecules depending on the alignment of the light beam with respect to an applied magnetic field,[4] has been shown to induce asymmetry in a chemical reaction.[5] It must be kept in mind that a static magnetic field is not enough to create chirality; however, a spin-polarized electron in motion has true chirality according to Barron's criterion because space inversion creates a distinguishable enantiomer whereas time inversion does not.[6]

The basic idea underlying this research, thus, is to explore the possible effects that could appear associated to the transfer of the spin-polarized electrons provided by a solid magnetic surface to chiral molecules adsorbed onto it, as a means to obtain enantioselectivity. Considerable evidence exists nowadays demonstrating the spin filtering effect of chiral molecules. Large asymmetries have been observed in the scattering of spin-polarized electron beams from films of purely organic chiral molecules.[7] Furthermore, unpolarized electrons have been found to become strongly spin-polarized upon crossing chiral DNA layers,[8] and later work by the authors has also shown that similar effects can be observed in electrons transmitted through thin layers of non-helical chiral molecules.[9] Spin-selective electron transmission has been detected between metallic substrates and adsorbed chiral molecules,[10–12] and spin-polarized electrons can also influence the kinetics of certain chemical reactions inducing the appearance of enantiomeric excess.[13]

2. Experimental

Two different types of chiral molecules were employed for the experiments reported here, each one with its corresponding enantiomers. 1,2-Diphenyl-1,2-ethanediol (DPED) possesses two chiral centers located at the two carbon atoms of the ethane chain. Its two enantiomers, (*R*,*R*)- and (*S*,*S*)-DPED are shown in Fig. 1. This molecule binds readily to Co through its –OH groups but physisorbs weakly on Cu. (1,2)-Diphenylethylenediamine (DPEDA), on the other hand, has a very similar atomic configuration as can be seen in Fig. 1, but the hydroxyl groups are substituted by amines ($–NH_2$) which form strong bonds with Cu at room temperature. Both compounds were purchased from Sigma-Aldrich and used without further purification; the purity degrees quoted by the supplier are 99% for DPED and 98% for DPEDA.

The experiments were carried out in all cases under ultra high vacuum (UHV) conditions. The Cu(100) single-crystal was cleaned by means of cycles of Ar^+ bombardment (~2 $\mu A/cm^2$) and thermal annealing at 900 K. The surface crystallinity and cleanliness was checked by means of low-energy electron diffraction (LEED) and spectroscopy measurements: either X-ray absorption (XAS) at the carbon K-edge or Auger electron spectroscopy (AES). Co was sublimated from a high-purity rod (99.995%) heated by electron bombardment (1 keV, 18 W). The chiral organic molecules were evaporated from Knudsen cells equipped with glass crucibles heated by direct current. All depositions were carried out *in situ* with the sample at room temperature. DPED has a melting temperature of ~421 K, but due to its low vapor pres-

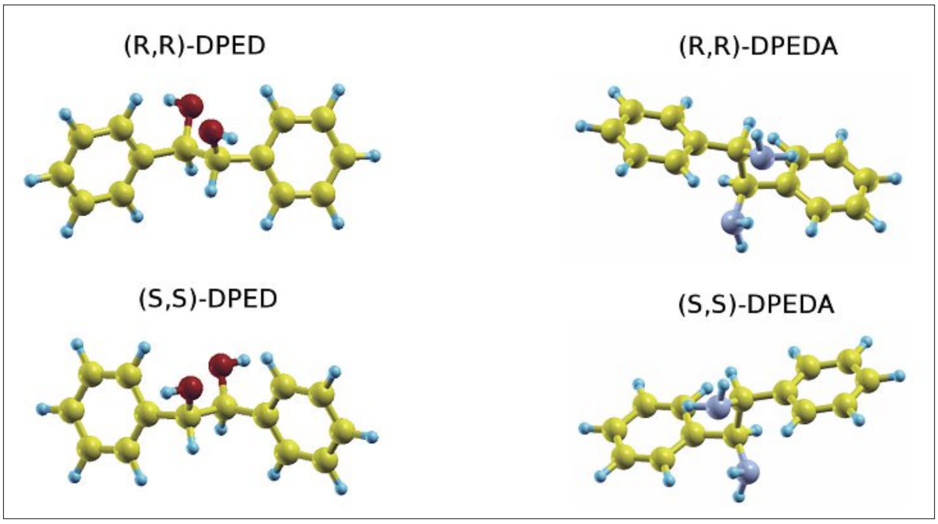

Fig. 1. Atomic configurations of the enantiomers of DPED and DPEDA. For DPED the red spheres represent the O atoms. For DPEDA, the large blue spheres correspond to the N atoms.

sure it was found that heating the crucible to 300 K was enough to produce a partial pressure in the 10^{-8} mbar range in the UHV chamber. The melting point of DPEDA is even lower (~353 K), and it was not necessary to heat the crucible containing the molecules; opening the valve separating the evaporator from the vacuum chamber was enough to obtain the desired exposure.

Co grows layer-by-layer on Cu(100) adopting initially the *fcc* structure and forming films with high structural quality and low roughness.[14] The magnetic properties of *fcc* Co films on Cu(100) are well known;[15] they have in-plane magnetization with large domains and high remanence. The deposited thicknesses are determined by means of XAS or AES, depending on the experimental system being used; films of at least 2 molecular layers (ML) have been used for these experiments to ensure that their Curie temperature would be above 300 K, so that the films remain magnetized during the measurements.[16]

The calibration of the adsorbed molecular film thicknesses presented in Section 3.1 was carried out at the home laboratory in Madrid using X-ray photoemission spectroscopy (XPS). The experimental system is equipped with a monochromatic aluminum anode producing photons of 1486.7 eV (Al K_α line) and a hemispherical energy analyzer (SPHERA-U7) with its pass energy set to 20 eV to have a resolution of 0.6 eV. The core levels energies are calibrated with respect to the Fermi edge and the Cu $2p_{3/2}$ peak of the clean Cu(100) substrate (binding energy of 932.3 eV).[17]

XAS experiments were conducted in total electron yield (TEY) mode and normal X-ray incidence with linearly polarized light at the surface science UHV station of beamline I1011 of the MAX-lab synchrotron in Lund, Sweden.[18] This experimental system consists of an upper preparation chamber where all the depositions were performed and a lower chamber where the XAS measurements took place. The samples were magnetized after deposition by applying current pulses to a set of rotatable coils that provide fields up to 600 G. Photoemission experiments have been carried out at the home laboratory in Madrid and also at synchrotron facilities: the I3 beamline of MAX-lab and CASSIOPEE of Soleil (France). In these two latter cases the spin-resolved photoemission stations were used, although for the results discussed in this paper only the integrated photoemitted intensities are considered. In the experiments carried out at the synchrotron UV light was used in a linear vertical polarization state. The photoemission spectra were collected under normal emission geometry in all cases. In order to minimize radiation damage to the molecular layers the irradiated area of the sample was periodically changed during the measurements.

3. Results and Discussion

3.1 *XPS Calibration of DPED Film Thickness on Co/Cu(100)*

The adsorption of DPED on Co/Cu(100) has been investigated by means of X-ray photoemission spectroscopy (XPS). The deposited thickness has been characterized by measuring the evolution of the integrated intensity of the C 1s peak as a function of exposure. The data corresponding to (*R*,*R*)-DPED are presented in Fig. 2a; the (*S*,*S*)-DPED enantiomer shows a similar behavior. It can be seen how the adsorption proceeds rapidly at the beginning, as the first DPED molecules arrive at the clean Co surface, while at the same time the signal corresponding to the Co 2p levels decreases accordingly as a result of the attenuation caused by the molecular overlayer. With increased exposure the sticking coefficient (slope of the C 1s curve) gradually decreases until a saturation coverage is reached: no further molecules are condensed unless the substrate temperature (295 K in these experiments) is lowered.

Fig. 2b shows the result of a fit to the attenuation curve of the Co signal with a model based on the scattering probability of the photoemitted electrons. An electron mean free path of 11.15 Å was used for this calculation as derived from studies carried out on alkanethiol layers adsorbed on Au surfaces.[19] This fit yields a saturation thickness of about 5 Å, which is consistent with a molecular bilayer. From this analysis we conclude that our DPED films adsorbed on Co after a prolonged exposure

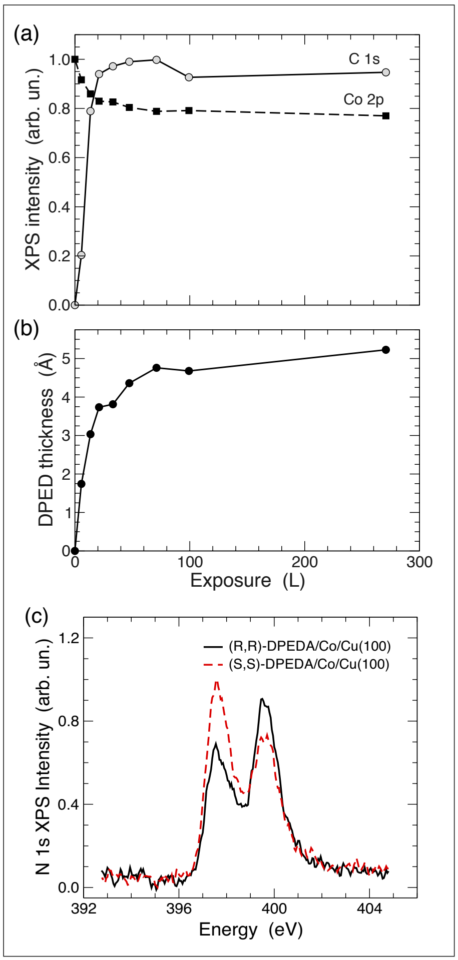

Fig. 2. XPS calibration of the thickness of (*R*,*R*)-DPED films adsorbed on Co/Cu(100). (a) Evolution of the C 1s and Co 2p photoemitted intensities as a function of exposure. (b) Thickness (in Ångström) of the DPED layer as derived from the fit to the attenuation of the Co 2p signal presented in (a). (c) Comparison of N 1s spectra for (*R*,*R*)- and (*S*,*S*)-DPEDA adsorbed on Co/Cu(100). Both spectra show a similar splitting with two components separated by ~2 eV, but the ratio of their intensities is inverted for one enantiomer with respect to the other.

consist of two monolayers of molecules: the first one, which is in direct contact with the metallic substrate and hence forms a stronger bond, and a second layer of molecules sitting on top of the former and more loosely bound to them. In order to obtain thicker films it was necessary to cool the sample below room temperature. A similar behavior has been found for DPEDA, also resulting in a saturation coverage of 2 ML at room temperature. A detailed account of the coverage calibration and a full STM study of the different ordered structures formed by DPEDA on Cu(100) is currently in preparation.[20]

It is interesting to note that some enantiosensitive effects are already observed in the XPS measurements. As perhaps the most striking example, Fig. 2c presents spectra acquired at the N 1s core level after the adsorption of (*R,R*)- and (*S,S*)-DPEDA on similar Co films grown on Cu(100). A clear splitting of nearly 2 eV is found in both cases, but the relative height of the two components is inverted when switching from one enantiomer to the other. Further work is currently underway to try to understand these observations.

3.2 *NEXAFS Measurements on DPED/Co/Cu(100)*

Near edge X-ray absorption fine structure (NEXAFS) spectra were measured at the C K-edge in TEY mode at beamline I1011 of MAX-lab. Besides the usual normalization of the measured intensities with respect to the beam current I_0, the raw spectra were also divided by the signal acquired from the clean Cu(100) surface in order to remove the spurious features caused by the X-ray absorption on the carbon deposits existing on the beamline mirrors. The Co film was magnetized in plane after absorbing the molecules and before starting the measurements. It was checked *in situ* by Co L-edge dichroic measurements that the Co film was in the ferromagnetic state after absorbing the molecules.

The spectra obtained after this double normalization process have been fitted using combinations of step and Voigt functions. These latter represent transitions bringing the C 1s electron from its initial state into different unoccupied orbitals. However, for the purpose of this paper we shall focus only on the analysis of the steps. These latter are observed in the NEXAFS spectra due to the photon excitation of the core electron to a continuum of final states. For a gas-phase molecule the occurrence of a continuum of final states in the NEXAFS spectra is expected once the X-rays have just sufficient energy to ionize the molecule. For solids and gas phase molecules only one step should be found at the ionization energy, representing transitions of the core electrons into the continuum, and often labelled the 'Vacuum Level' (VL) step.[21] The occurrence of the VL step is well known in the gas phase spectra as it corresponds to the C 1s state binding energy which can be measured by a photoemission experiment. The situation is more complex in the case of physisorbed or chemisorbed molecules. Due to the hybridization between the substrate and the molecular levels, an extra channel is available after photon excitation to the photoexcited C 1s electron to reach a continuum of final states, consisting of the density of empty final states due to the existence of the metallic substrate. Therefore, a second step may appear in the NEXAFS spectra directly linked with the hybridization of the metal with the molecule and the transition of the core electrons of the metal above the Fermi level. This is usually referred to as the 'Fermi Level' (FL) step.[21,22] The occurrence of this second step is well defined energetically. The FL step is observed at a lower energy versus the VL step, with an energy difference versus the VL step corresponding to the work function of the substrate. For weakly adsorbed molecules, a FL step with only a weak intensity is observed. As the FL step intensity is reflecting the hybridization strength between the molecular levels with the substrate ones, one expects to observe an increase in the intensity of the FL step versus the VL step, as the strength of the molecular binding to the substrate increases. Ultimately, for strong chemisorption only the FL level is observed, as in such a case the two systems, the substrate and the adsorbed molecule, are forming a single entity in terms of electronic structure. Several cases consistent with this picture of hybridization strength and the observation of a VL and FL steps are known in the literature.[21,23] Here we can use the previous observations in NEXAFS spectra to obtain an idea of the strength of the hybridization taking place between the orbitals of the DPED molecules and the Cu(100) and Co/Cu(100) surfaces, given the observation of a VL and a FL step in the DPED NEXAFS spectra.

The corrected carbon K-edge spectrum of the 2 ML thick (*R,R*)-DPED layer adsorbed on 3.4 ML Co/Cu(100) is shown in Fig. 3, where it is also compared with a film of the same enantiomer physisorbed on Cu; this latter experiment was carried out at 150 K since DPED does not lead to a stable adsorption state on Cu at room temperature. The red line superimposed to the data represents the fit to the experimental spectrum; it is obtained after adding up the different components also indicated in the graph. (*R,R*)-DPED is weakly chemisorbed on Co/Cu(001) since its Fermi level step at 283.8 eV is much lower than the VL step at 288.5 eV. In fact, its height is quite similar in both spectra.

It should be mentioned that the spectra presented here are the result of the accumulation of many iterations in order to improve the signal-to-noise ratio. Some effects of beam damage were observed after prolonged exposure of the molecular films to the X-rays; for this reason, the irradiated spot on the sample was changed periodically to minimize those alterations. In any case the damage observed resulted in moderate changes in the height of some of the peaks used in the fit (the ones represented with the Voigt functions and depicted with brown solid lines in Fig. 3b) but did not provoke significant changes in the height of the steps discussed here.

(*S,S*)-DPED molecules were evaporated onto 2.0 ML Co/Cu(001). The corresponding NEXAFS spectrum is depicted in Fig. 4, also in comparison with a measurement on a physisorbed film of the same enantiomer on Cu(100) at 150 K. In this case the steps are quite different depending on the substrate: the system adsorbed on Co presents a larger Fermi level step at 283.8 eV, implying that (*S,S*)-DPED chemisorbs on Co with a stronger hybridization than (*R,R*)-DPED.[21,23] A

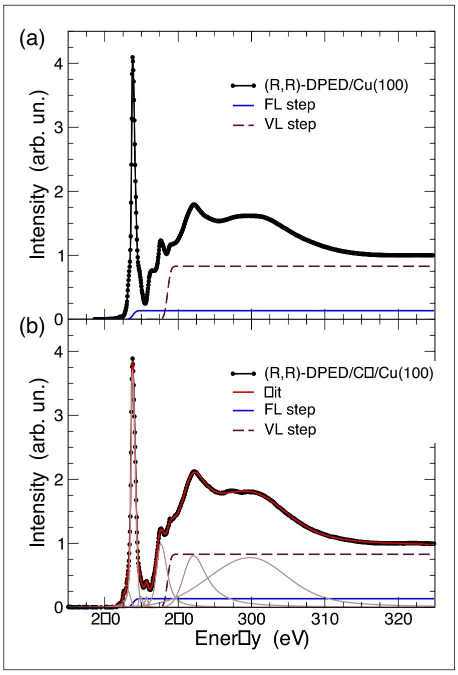

Fig. 3. Carbon K-edge NEXAFS spectra at normal incidence for (*R,R*)-DPED (a) physisorbed on Cu(100) at 150 K and (b) chemisorbed on 3.4 ML Co/Cu(100) at room temperature. In this latter spectrum the red solid line represents the fit achieved by combining the different contributions also shown in the plot. The individual peaks depicted with brown lines represent transitions of the core electron into empty molecular orbitals. The two steps (Fermi Level and Vacuum Level), in turn, correspond to transitions into the continuum as discussed in the text. The low intensity of the FL step for (*R,R*)-DPED on both Cu(100) and Co/Cu(100) is indicative of a weak adsorption.

quantitative estimate of the associated bonding energies will require a detailed theoretical analysis of the data. It is also remarkable that the relative height of the π* resonance at 283.8 eV with respect to the high-energy part of the spectrum is considerably reduced for (*S*,*S*)-DPED/Co in comparison with all the other cases. Such an effect could be due to a different orientation of the adsorbed molecules with respect to the incoming X-ray beam, but that would also imply some differences in the bonding of the two enantiomers with the substrate. Further theoretical and experimental work is needed to fully clarify these points.

3.3 *Valence Band Photoemission in DPEDA Films Adsorbed on Co/Cu(100)*

Ultraviolet photoemission spectroscopy (UPS) has been used to investigate the valence band region for DPEDA films deposited also on epitaxial Co layers grown on Cu(100). The UPS spectra presented in the following have been fitted with a model in which the background due to the secondary electrons is represented by a step function. This background can be approximated by a constant due to the large photon energy employed in these experiments (40 eV). Besides that, a set of Gaussians represent occupied states below E_F from which electrons are photoemitted. They are labelled with letters 'A' through 'F' for clarity.

Fig. 5 shows the UPS spectrum measured on a 6 ML-thick Co film epitaxially grown on Cu(100), with no molecules adsorbed on it. The film was magnetized in-plane after adsorbing the molecules and before starting the measurements. Since the purpose of this paper is to highlight the differences in the spectra that can be associated to the different chirality of the enantiomers while trying to eliminate other possible influences, we only report here data obtained for one orientation of the Co magnetization vector, which will be denoted as *positive*. We have also carried out the corresponding measurements for the *negative magnetization*, which show similar differences between the two enantiomers. These spectra are not presented here for the sake of brevity. As for the study of the influence of the sample magnetization (positive versus negative), it will be the subject of a future publication.

The relatively high background of secondaries is justified by the high density of states near the Fermi level, characteristic of a magnetic metal like Co. Three relatively narrow peaks A, B and C can be identified below E_F, at binding energies of 0.32, 0.71 and 1.24 eV respectively. The component closest to the Fermi level corresponds to the minority sub-band.[24] At higher binding energies other broader peaks can be observed at –2.7 (D), –5.1 (E) and –7.0 eV (F). The small feature at –2.8 eV indicated by means of an arrow corresponds to electrons emitted from the *d*-band of the Cu substrate, which can cross the Co layer due to its small thickness.

Fig. 6 presents an analogous UPS spectrum measured in the same energy range, after covering the Co film with a saturated (*i.e.* 2 ML thick) layer of (*R*,*R*)-DPEDA. Several significant changes can be observed with respect to the measurement on the clean Co surface. In the first place, the peak in the integrated intensity right below E_F has become sharper; the fit to the spectrum reveals that component A,

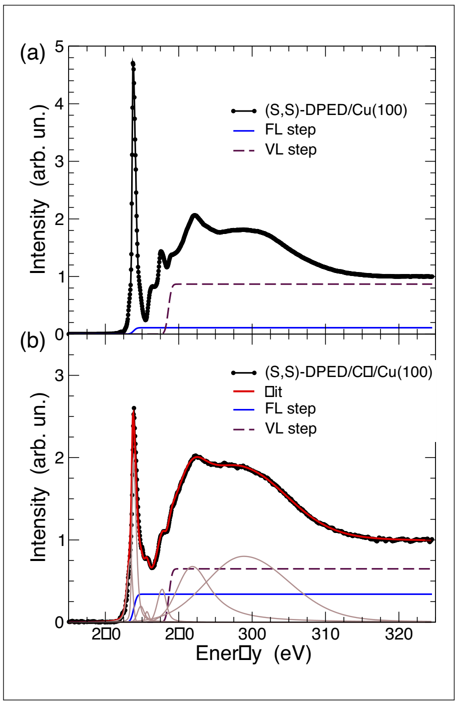

Fig. 4. Carbon K-edge NEXAFS spectra at normal incidence for (*S*,*S*)-DPED (a) physisorbed on Cu(100) at 150 K and (b) chemisorbed on 2 ML Co/Cu(100) at room temperature. As in Fig. 3, the red solid line represents the fit to the spectrum measured on Co/Cu(100) with the components also shown in the graph. In this case the FL step shows a substantially higher intensity for (*S*,*S*)-DPED adsorbed on Co/Cu(100), indicating that the hybridization between the surface and the molecular orbitals is stronger on Co than on Cu, and also than for (*R*,*R*)-DPED on a similar Co/Cu(100) substrate.

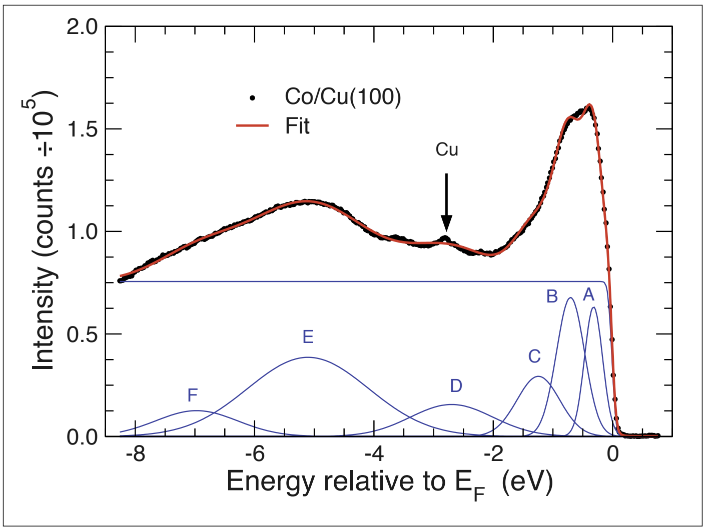

Fig. 5. Fit (red line) to the UPS spectrum measured at normal emission on a 6 ML Co film epitaxially grown on Cu(100). The experimental data are depicted with black dots. The different components used in the fit are also depicted with blue lines and labelled as described in the text.

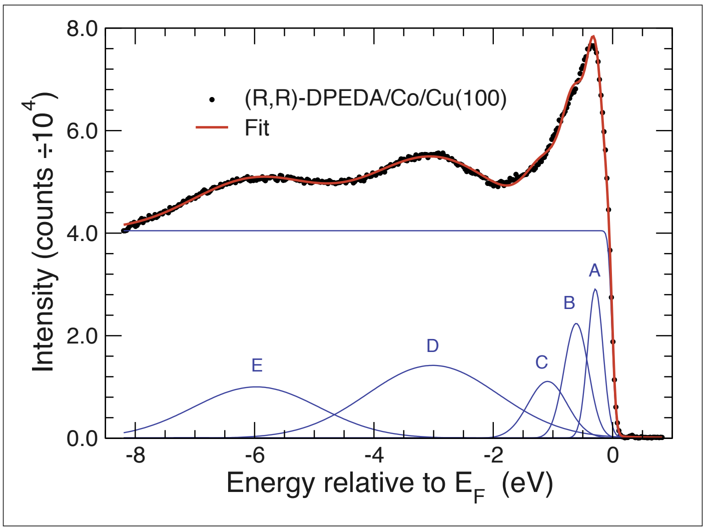

Fig. 6. Fit (red line) to the UPS spectrum measured at normal emission on 2 ML (*R*,*R*)-DPEDA adsorbed on 6 ML Co/Cu(100). The experimental data are depicted with black dots. The different components used in the fit are also depicted with blue lines and labelled as described in the text.

which lies closest to the Fermi energy, has now a higher intensity with respect to the other two, B and C. This would imply that either there has been a transfer of charge from the adsorbed molecules into that minority band of Co (which had more empty states before the adsorption) or, more likely given the characteristics of the Co-N bonds, some charge has been transferred toward the molecules, preferentially from the other states lying below in energy, partially emptying them. Besides, all three components are slightly shifted upwards in energy, the largest shift being +0.15 eV for peak C. The rest of the spectrum also shows substantial differences in comparison to that of clean Co. The broad peaks are shifted to higher binding energies (to –3.0 and –6.0 eV for D and E) and their relative intensities also change: the first one increases substantially while the second one decreases and the third one (F) practically disappears. Finally, the traces of Cu *d* electrons are no longer visible after coating the Co film with the molecular layer.

Next we focus on the analysis of the UPS spectrum measured on a film of (*S*,*S*)-DPEDA adsorbed on an analogous film of Co, which is presented in Fig. 7. The difference with the one obtained for the (*R*,*R*) enantiomer is striking. In the first place, the relative intensity of the secondaries is much higher with respect to the peaks. This observation can be a hint of an enhanced probability of scattering of the photoelectrons upon crossing the molecular layer, supporting recent claims that this type of chiral molecular films can act as spin filters.[8,9] Besides, the energy shifts of the different components are very different: in particular, peak B moves upwards by 0.16 eV and component C by as much as 0.46 eV, suggesting that these electronic states are strongly modified by the bonding with the molecular orbitals. The lower lying states D, E and F, on the other hand, are much less perturbed: they appear at practically the same energies as in the clean Co spectrum of Fig. 5 and only some differences in their relative intensities can be remarked.

Although these results are still preliminary, they unequivocally suggest that the bonding of the DPEDA molecules on the spin-polarized Co substrate shows significant enantiosensitive differences that could be exploited for instance for spintronic applications or for chiral resolution of racemic compounds.[25] Further work is in progress to try to identify the link between the chiral symmetry of the molecules and their bonding with spin-polarized substrates.

4. Conclusions

The adsorption of chiral organic molecules on a ferromagnetic substrate has been investigated by surface science techniques carried out under ultra high vacuum. Synchrotron-radiation-based electron spectroscopies allow us to characterize both the substrate's and molecular electronic states and to detect possible changes provoked by the molecule–surface bonding. In this way, significant differences associated to the molecule's helicity have been detected. With the two chiral molecules employed in these studies, DPED and DPEDA, a stronger interaction is observed between the (*S*,*S*) enantiomer and the spin-polarized Co substrate than for its (*R*,*R*) counterpart. This behavior might be related to the recently reported CISS (chirality induced spin selectivity) effect, and it can have long-ranging implications for applications such as molecular spintronics or chiral resolution of racemic compounds.

Acknowledgements

The authors are grateful to the MAX-lab and Soleil staff for their help during the execution of these experiments. This work has been financed in Spain by the Mineco through Grants MAT2013-47869-C4-3-P and FIS2016-74893-P and in Poland by the National Science Centre through Grant 2011/03/D/ST3/02654. Additional support for our experiments at the synchrotron through the European CALIPSO Programme and the Carl Tryggers foundation for Science Research (contract CTS 16:32) is also acknowledged.

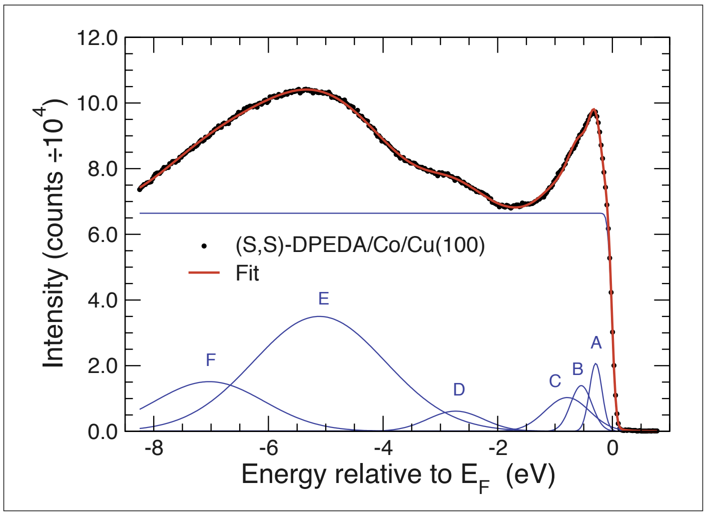

Fig. 7. Fit (red line) to the UPS spectrum measured at normal emission on 2 ML (*S*,*S*)-DPEDA adsorbed on 6 ML Co/Cu(100). The experimental data are depicted with black dots. The different components used in the fit are also depicted with blue lines and labelled as described in the text.

Received: April 25, 2018

[1] S. F. Mason, *Nature* **1984**, *311*, 19.

[2] L. D. Barron, *J. Am. Chem. Soc.* **1986**, *108*, 5539.

[3] L. D. Barron, J. Vrbancich, *J. Mol. Phys.* **1984**, *51*, 715.

[4] a) G. Wagnière, A. Meier, *Chem. Phys. Lett.* **1982**, *93*, 78; b) G. L. J. Rikken, E. Raupach, *Nature* **1997**, *390*, 493.

[5] G. L. J. Rikken, E. Raupach, *Nature* **2000**, *405*, 932.

[6] L. D. Barron, *Chirality* **2012**, *24*, 879.

[7] K. Ray, S. P. Ananthavel, D. H. Waldeck, R. Naaman, *Science* **1999**, *283*, 814.

[8] B. Göhler, V. Hamelbeck, T. Z. Markus, M. Kettner, G. F. Hanne, Z. Vager, R. Naaman, H. Zacharias, *Science* **2011**, *331*, 894.

[9] M. Á. Niño, I. A. Kowalik, F. J. Luque, D. Arvanitis, R. Miranda, J. J. de Miguel, *Adv. Mater.* **2014**, *26*, 7474.

[10] V. Kiran, S. R. Cohen, R. Naaman, *J. Chem. Phys.* **2017**, *146*, 092302.

[11] F. Tassinari, D. R. Jayarathna, N. Kantor-Uriel, K. L. Davis, V. Varade, C. Achim, R. Naaman, *Adv. Mater.* **2018**, 1706423.

[12] M. Kettner, V. V. Maslyuk, D. Nürenberg, J. Seibel, R. Gutierrez, G. Cuniberti, K.-H. Ernst, H. Zacharias, *J. Phys. Chem. Lett.* **2018**, *9*, 2025.

[13] R. A. Rosenberg, D. Mishra, R. Naaman, *Angew. Chem. Int. Ed.* **2015**, *54*, 1.

[14] a) J. J. de Miguel, A. Cebollada, J. M. Gallego, S. Ferrer, R. Miranda, C. M. Schneider, P. Bressler, J. Garbe, K. Bethke, J. Kirschner, *Surf. Sci.* **1989**, *211/212*, 732; b) C. M. Schneider, P. Bressler, P. Schuster, J. Kirschner, J. J. de Miguel, R. Miranda, S. Ferrer, *Vacuum* **1990**, *41*, 503.

[15] J. J. de Miguel, A. Cebollada, J. M. Gallego, R. Miranda, C. M. Schneider, P. Schuster, J. Kirschner, *J. Magn. Magn. Mater.* **1991**, *93*, 1.

[16] C. M. Schneider, P. Bressler, P. Schuster, J. Kirschner, J. J. de Miguel, R. Miranda, *Phys. Rev. Lett.* **1990**, *64*, 1059-1062.

[17] D. Maccariello, M. Garnica, M. Á. Niño, C. Navío, P. Perna, S. Barja, A. L. Vázquez de Parga, R. Miranda, *Chem. Mater.* **2014**, *26*, 2883.

[18] I. A. Kowalik, G. Öhrwall, B. N. Jensen, R. Sankari, E. Wallén, U. Johansson, O. Karis, D. Arvanitis, *J. Phys.: Conf. Ser.* **2010**, *211*, 012030.

[19] C. L. A. Lamont, J. Wilkes, *Langmuir* **1999**, *15*, 2037.

[20] R. P. Palacios et al., in preparation.

[21] J. Stöhr, 'NEXAFS Spectroscopy', Springer, **1996**.

[22] D. A. Outka, J. Stöhr, *J. Chem. Phys.* **1988**, *88*, 3539.

[23] W. Wurth, J. Stöhr, P. Feulner, X. Pan, K. R. Bauchspiess, Y. Baba, E. Hudel, G. Rocker, D. Menzel, *Phys. Rev. Lett.* **1990**, *65*, 2426.

[24] a) C. M. Schneider, J. J. de Miguel, P. Bressler, P. Schuster, R. Miranda, J. Kirschner, *J. Electron Spectrosc. Relat. Phenom.* **1990**, *51*, 263; b) C. M. Schneider, P. Schuster, M. Hammond, H. Ebert, J. Noffke, J. Kirschner, *J. Phys.: Condens. Matter* **1991**, *3*, 4349.

[25] K. Banerjee-Ghosh, O. Ben Dor, F. Tassinari, E. Capua, S. Yochelis, A. Capua, S.-H. Yang, S. S. P. Parkin, S. Sarkar, L. Kronik, L. T. Baczewski, R. Naaman, Y. Paltiel, *Science* **2018**, 10.1126/science.aar4265.